forests

MDPI

Article

Reconstructing 450 Years of Pollarding Events in Spanish Deciduous Oak Woodlands Using Machine Learning

Alba Sanmiguel-Vallelado, Gabriel Sangüesa-Barreda, Miguel García-Hidalgo, María Encarnación Coca and José Miguel Olano *

Instituto Universitario de Investigación en Gestión Forestal Sostenible (iuFOR), Escuela Universitaria de Ingeniería de la Industria Forestal, Agronómica y de la Bioenergía (EiFAB), Universidad de Valladolid, Campus Duques de Soria sn, 42004 Soria, Spain; alba.sanmiguel@uva.es (A.S.-V.); gabriel.sanguesa@uva.es (G.S.-B.); miguel.garcia.hidalgo@uva.es (M.G.-H.); mariaencarnacion.coca@uva.es (M.E.C.)
* Correspondence: josemiguel.olano@uva.es

Abstract: Pollarding, the practice of pruning tree branches at a specific height, has been crucial for managing open forests in Europe. This practice has supported the persistence of highly biodiverse open woodlands featuring ancient trees. Understanding historical management patterns is essential for interpreting past socioeconomic conditions and developing strategies to mimic traditional practices for biodiversity conservation. Current methods for reconstructing past management in pollarded forests often rely on techniques for large-scale forest disturbances, which may be suboptimal for detecting short-term perturbations like pollarding. To address this gap, we applied a random forest algorithm to detect pollarding events using tree-ring traits, reconstructing the multi-centennial management history of four deciduous oak *dehesas* in northern Spain. Our analysis revealed that short-term changes in latewood were the most reliable indicator of pollarding events. Pollarding typically reduced latewood production for about three years, with the most pronounced declines occurring toward the end of the pollarding effect period. Pollarding patterns underwent a major shift starting in the last third of the 20th century. Key historical decades of both high and low pollarding pressure were consistently observed across the studied *dehesas*. These findings enhance our understanding of these unique ecosystems and offer critical insights for their conservation.

Keywords: *Dehesas*; dendrochronology; open woodlands; *Quercus* spp.; random forest

Citation: Sanmiguel-Vallelado, A.; Sangüesa-Barreda, G.; García-Hidalgo, M.; Coca, M.E.; Olano, J.M. Reconstructing 450 Years of Pollarding Events in Spanish Deciduous Oak Woodlands Using Machine Learning. *Forests* **2024**, *15*, 2090. https://doi.org/10.3390/15122090

Academic Editors: Yu Liu and Giorgio Vacchiano

Received: 7 October 2024
Revised: 12 November 2024
Accepted: 21 November 2024
Published: 26 November 2024

1. Introduction

Pollarding is a traditional forestry management practice that involves removing the upper part of a tree trunk through systematic pruning of branches at varying intensities [1]. For centuries, this practice has shaped agrosilvopastoral landscapes across Europe by maintaining open woodlands [2,3]. Pollarding provided a sustainable means for traditional societies to obtain essential provisioning services, such as poles for construction, fodder for livestock, firewood, and charcoal [4–6].

Oak trees have been subjected to pollarding in the Iberian Peninsula's open woodlands, known as *dehesas* (defenses), since at least the Early Middle Ages [7]. In the western and southwestern Iberian Peninsula, *dehesas* are dominated by xerophilous evergreen species such as *Quercus ilex L.* and *Q. suber* L. conforming large private estates. By contrast, in the more humid regions of northern and central Spain, *dehesas* are dominated by deciduous oaks, including *Q. faginea* Lam. and *Q. pyrenaica* Willd. [6], and are historically associated with village commons. While large private *dehesas* continue to be regularly pollarded [8,9], management in village commons has declined sharply, often leading to tree decline [10].

Iberian *dehesas* are recognized as crucial for both cultural heritage preservation [11,12] and biodiversity maintenance [13,14]. Traditional pollarding, which prevents tree cutting and induces periodic reductions in growth, results in trees with longer lifespans [15,16].

This practice led to a remarkable abundance of old trees in pollarded oak woodlands [17]. Dendrochronological studies of these trees enable the reconstruction of the long-term human–tree interactions [18–20], providing deeper insights into these unique ecosystems and their conservation.

Pollarding generates a complex signal in tree growth, involving multiple tree-ring variables [21,22]. This practice causes a sharp and significant reduction in tree-ring width immediately following the event [23]. This decrease is most pronounced in latewood width, while earlywood width initially remains stable. Consequently, the proportion of earlywood in the tree ring increases markedly due to the reduction in latewood [20,21]. Over the following years, tree-ring width gradually recovers [20–22]. Most studies detecting pollarding events in tree growth series use techniques developed for identifying forest disturbances [10,18–20,24], such as the radial-growth averaging criteria. This approach has been applied in most cases using 10-year analysis windows, which may be ineffective for identifying short-term growth reductions, such as those caused by pollarding [10,18,19,24].

Anomaly detection, such as identifying pollarding in tree-ring data series, presents several challenges, primarily due to the variability of the signals left in the wood, which can result in shorter or longer traces with varying magnitudes. The use of machine learning techniques can facilitate the identification of such growth anomalies, as they can detect complex patterns, handle nonlinear data, manage high dimensionality, and address missing values, offering substantial advantages over traditional statistical methods [25–28]. We utilized machine learning-based methods to develop a model for reconstructing pollarding events from tree-ring data. We investigated the integration of (1) additional tree-ring traits beyond ring width and (2) shorter time windows for creating predictor variables to identify pollarding events. The objectives of this study were the following: (i) to develop a method for detecting pollarding events using early and latewood width time series with supervised machine learning techniques, and (ii) to reconstruct historical forest management by analyzing the recurrence, severity, and synchrony of pollarding events at the studied sites. The findings of this study inform the management practices that have sustained these forests over the past four centuries, practices that have been pivotal in their survival to the present day. This historical knowledge can guide the re-establishment of management patterns essential for ensuring the conservation and resilience of these forests into the future.

2. Materials and Methods

2.1. Study Sites and Field Sampling

We selected four large open communal woodlands (43–2793 hectares) in north-central Spain, dominated by deciduous oak trees traditionally subjected to pollarding. Pollarding took place during winter when the trees were in a dormant state. These woodlands are situated at an average altitude of 1101 m a.s.l. (Figure 1; Table 1) and experience a continental climate with Atlantic influences, featuring freezing winters, hot summers, and significant diurnal and seasonal temperature variations. The annual precipitation averages 543 $\pm$ 28 mm, with a summer water deficit. The parent material is predominantly sandstone, with gravel and marl present at Rioseco. The Vilviestre site is dominated by *Quercus faginea*, with scattered *Q. pyrenaica*. The Valonsadero site is mainly populated by *Q. pyrenaica*, with occasional *Q. faginea* and, less commonly, *Q. petraea* (Matt.) Liebl. The Arguijo site is characterized by prevalent *Q. pyrenaica*, with scattered *Q. petraea* and *Fagus sylvatica* L. Finally, the Rioseco site is dominated by *Juniperus thurifera* L., with minor occurrences of *Q. faginea* and *Q. pyrenaica*.

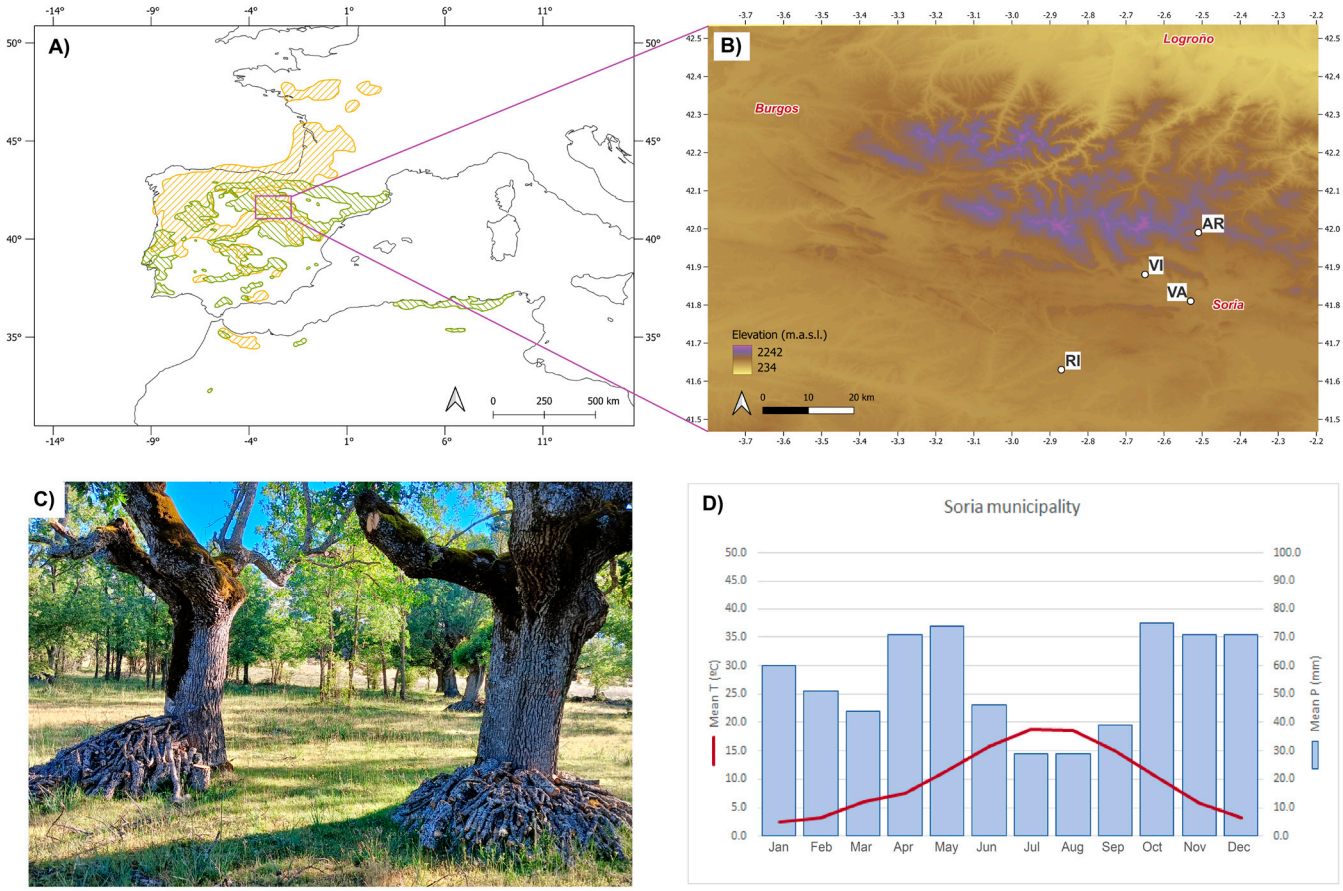

Figure 1. (**A**) Distribution range of the main sampled species, *Q. pyrenaica* and *Q. faginea* [29]. (**B**) Locations of the four studied pollarded woodlands (AR, RI, VA, VI), with surrounding major cities in Spain. Digital Terrain Model source: PNOA 1:200,000 ETRS89 HU30 Soria. (**C**) Picture of recently pollarded *Quercus pyrenaica* oaks at the Vilviestre site. (**D**) Thirty-year ombrothermal diagram of the municipality of Soria to represent the regional context (period: 1981–2020; data source: Spanish State Meteorological Agency).

Table 1. Characteristics of the four study sites and dendrochronological features.

Site (Code)	Lat (°N)	Long (°W)	Elevation (m a.s.l.)	Area (ha)	N Trees x Species	Time Span	Mean Series Length (Years)	Mean Ring Width ± SD (mm)	Mean AR1	Mean SI	EPS
Vilviestre (VI)	41.88	−2.65	1069	270	6 *pyr*, 45 *fag*	1538–2022	371	0.60 ± 0.32	0.61	0.51	0.96
Valonsadero (VA)	41.81	−2.53	1040	2793	54 *pyr*	1715–2022	210	1.12 ± 0.68	0.60	0.54	0.97
Arguijo (AR)	41.99	−2.51	1290	43	40 *pyr*, 3 *pet*	1588–2022	266	1.04 ± 0.59	0.67	0.48	0.94
Rioseco (RI)	41.63	−2.87	1003	100	9 *pyr*, 43 *fag*	1855–2022	151	1.31 ± 0.64	0.65	0.63	0.98

Abbreviations: latitude (Lat); longitude (Long); pyr (*Q. pyrenaica*); fag (*Q. faginea*); pet (*Q. petraea*); standard deviation (SD); first-order autocorrelation (AR1); series intercorrelation (SI); expressed population signal (EPS).

We sampled the study sites between October 2022 and April 2023. One core per tree was extracted at 1.3 m above ground level using a Pressler increment borer (Häglof, Sweden). This approach optimizes the number of trees sampled with the same effort. Low variability in individual tree growth, attributed to minimal slope and limited competition among trees, allowed for effective cross-dating with only one core per tree [17]. Trees were sampled at regular intervals within each woodland to minimize synchronous management effects. In total, 200 trees were sampled. The sampled trees included 109 *Q. pyrenaica*, 88 *Q. faginea*, and 3 *Q. petraea*.

2.2. Sample Processing

Tree cores were air-dried, mounted onto wooden supports, and sanded with progressively finer sandpaper grades from 80 to 800 grit. They were then digitized using a CaptuRING device [30] equipped with a Tokina Macro 100 F2.8 lens on a Nikon D7500 camera and PTGui v8.3 software (New House Internet Services BV, Rotterdam, The Netherlands), achieving a resolution of 5897 dpi. Subsequently, CooRecorder v9.6 software (Cybis Elektronik & Data AB, Saltsjöbaden, Sweden) was used to manually measure tree ring, earlywood, and latewood widths for each year (tree ring) with a precision of 0.004 mm. Cross-dating, error correction, and chronology generation were performed using the dplR package [31] in the R environment [32].

2.3. Automatic and Supervised Detection of Pollarding Events

We trained a random forest algorithm [33] for the automatic detection of pollarding events using the R package randomForest [34]. Random forest is a decision tree-based method that generates and aggregates the results of multiple trees using bootstrap samples of the input data, improving accuracy and reducing the risk of overfitting [35]. Random forest methods have been successfully applied to tree ring datasets [25,27,36,37].

The training dataset consisted of 20 trees from each of the four sampled sites (N trees = 80) and 331 visually identified pollarding events. Pollarding events, classified as a value of 1 in the response variable, were identified by an abrupt reduction in latewood width lasting at least 3 years, followed by a delayed and gradual recovery over several years [20–22]. This pattern differentiates pollarding from other growth anomalies such as drought events, as oak growth is highly dependent on water availability [17]. Years without evidence of pollarding were classified as 0 in the response variable, while years with uncertainty were not assigned to any class (NA).

A range of predictor variables, calculated for each year based on tree-ring data (Table S1), was included in the training dataset. These variables were based on total ring width (RW), earlywood width (EW), and latewood width (LW). One set of predictor variables include the EW/RW and LW/RW ratios, which measure the percentage of EW and LW relative to the RW for the focal year, as well as their mean values for the subsequent 1 to 10 years. Another group of predictor variables was created using the radial-growth averaging criteria [38]. This method was applied to RW, EW, LW, EW/RW ratio, and LW/RW ratio variables. It involves calculating the percentage of growth change (PGC) for each variable based on its mean value in the pre-disturbance period (1 to 10 years, including the focal year) (M1) and its mean value in the post-disturbance period (1 to 10 years) (M2). The formula used is as follows:

$$\text{PGC}\ (\%) = [(\text{M2} - \text{M1})/\text{M1}] \times 100 \quad (1)$$

The model was trained applying a random forest binary classification algorithm on the complete training dataset [34]. It was unnecessary to optimize the algorithm's complexity, as random forests are known for their robustness against overfitting, and the need for hyperparameter tuning is limited to very specific cases [39]. The number of samples to be selected from each category of the response variable was balanced when constructing each tree in the model, with the total number of pollarding events included and three times the number of non-pollarding events. Due to the spatio-temporal dependence of the data, the model's predictive ability was estimated using spatio-temporally independent block cross-validation, considering site x century combinations. The model's performance was assessed using various metrics: Kappa, accuracy, F1-score, sensitivity, specificity, and area under the receiver operating characteristic curve (AUC-ROC) (Table 2). Kappa measures the level of agreement between predicted and actual classifications adjusting for the agreement that could occur by chance, accuracy measures correct predictions, F1-score assesses prediction accuracy for each class, sensitivity measures true positive identification, specificity measures true negative identification, and AUC-ROC quantifies

the model's ability to distinguish between classes across all threshold levels. Predictor variable importance was assessed using the Gini index, which plays a crucial role in building an effective decision tree by guiding the selection of optimal splitting features. By minimizing the Gini index at each node, the decision tree progressively separates data points into different classes, leading to accurate predictions at the terminal leaves. The Gini index varies between 0 and 1, where 0 represents purity of the classification and 1 denotes random distribution of elements among various classes. A Gini index of 0.5 shows an equal distribution of elements across some classes.

Table 2. Performance metrics and the ten most important variables in the random forest model performed.

Performance Metric	Value	Top 10 Predictor Variables	Mean Decrease Gini
Kappa	0.62	PGC3_L	46
Sensitivity	0.85	PGC2_L	41
Specificity	0.95	PGC3_ratioL	36
AUC	0.97	PGC4_L	29
		PGC1_L	26
		PGC2_ratioL	24
		PGC4_ratioL	20
		PGC1_ratioE	19
		PGC3_ratioE	18
		PGC1_ratioL	16

Abbreviations: AUC, area under the curve. Acronyms for predictor variables and their calculations can be found in Table S1.

The model was used to identify pollarding events in additional trees and in periods not included in the training data. When events were assigned to two consecutive years within the same growth suppression period, only the first event was retained.

2.4. Discrimination of Pollarding Events and Drought Events

We calculated the standardized precipitation evapotranspiration index (SPEI) for each sampling site for the period from 1901 to 2022 using the R SPEI package [40]. SPEI is a multiscalar drought index [41]. Monthly precipitation and temperature gridded data ($0.5^\circ \times 0.5^\circ$) were sourced from the Climate Research Unit, University of East Anglia (https://crudata.uea.ac.uk/ (accessed on 10 May 2024); 4.07 version; [42]). The SPEI used at each site corresponds to the lag and month with the highest correlation with the mean latewood width index chronology (Table S2). Moderate and severe droughts were defined as years where the SPEI value was ≤ -0.84 or ≤ -1.28, respectively [43,44]. Severe droughts are prone to causing long-lasting effects on growth and potentially being mistaken for pollarding events. The first criterion for excluding an event was if the year following the event exceeded the mentioned SPEI threshold for severe droughts. The second criterion was if the first year after the event exceeded the SPEI threshold for moderate droughts, and a severe drought occurred in the second year. These criteria were used both for the selection of events for model training and for filtering the events predicted by the model.

2.5. Analysis of Tree Management Patterns

The pollarding events identified by the model were used to reconstruct tree management patterns. First, the initial 5 years of each tree's growth were excluded due to insufficient prior data to assess pollarding events. For site-level analyses, only periods with at least four available trees were considered. Three parameters were considered for reconstructing tree pollarding: recurrence, severity, and synchrony.

Plot pollarding recurrence was calculated as the mean return period. It was computed at the site level within a specific moving time window (10-year periods, lagged by 1 years) following [45]. Pollarding severity was calculated for each event as the num-

ber of years elapsed until the first year in which recovery was observed, marked by an abrupt positive growth change. The annual latewood production rate remains negative for several years after the event and then turns positive when recovery starts, exceeding a 50% threshold [46,47]. If this threshold is not surpassed before the next pollarding event, recovery is defined as the first year in which the rate becomes positive, regardless of its magnitude. We excluded pollarding events with a severity of less than 2 years from the subsequent analyses due to their difficulty in distinguishing from drought events and their relatively mild impact. Pollarding synchrony was calculated at site level following [45]. This method generates a metric that compares the actual temporal distribution of pollarding events with the most synchronous potential distribution within a specific moving time window (10-year periods, lagged by 1 year).

Differences in pollarding recurrence, severity, and synchrony among sites or time periods were tested using non-parametric tests due to non-normal data distribution (Shapiro–Wilk test: $p < 0.05$). The Kruskal–Wallis test (H statistic) [48] was applied, with post hoc comparisons between groups performed using Dunn test (Z statistic) [49]. Temporal trends in pollarding recurrence, severity, and synchrony at each site were assessed using the Mann–Kendall test [50,51], and the Theil–Sen's slope estimator [52] was used to determine trend magnitude. Trend analyses were conducted using the zyp package [53] in R environment [32], incorporating a trend-free prewhitening method to account for serial autocorrelation.

2.6. Radial-Growth Responses to Pollarding

We assessed the effect of pollarding on different tree growth components (RW, EW, and LW). We evaluated changes in these components in the years following the event (Year 1, 2, 3, etc.) compared to pre-event conditions (Year 0). Additionally, we analyzed the year-on-year change in these components throughout the period where pollarding effects were observed. The Wilcoxon test for paired samples was used to determine whether the differences in these parameters between years were statistically significant.

We employed regression trees to identify different pollarding types based on the changes they produced in RW, EW, and LW compared to pre-event conditions. The existence of homogeneous groups was determined based on three explanatory variables: (1) time since the previous pollarding event, (2) severity of the pollarding event, and (3) time since recovery from the previous pollarding event. The Dunn test was used to assess statistical differences among the identified pollarding groups.

3. Results

3.1. Performance of the Semi-Automated Process of Pollarding Events Detection

The random forest model showed an overall Kappa of 0.62. Its ability to correctly identify non-pollarding cases (specificity = 0.95) was higher than for pollarding events (sensitivity = 0.85), reflecting the conservative nature we intentionally imparted to the model. Traits related to latewood were the most accurate predictors, particularly for short time windows (1–5 years).

Only 9% of the 669 events identified between 1900 and 2018 corresponded with or were influenced by severe droughts. This impacted 35 of the 619 events in the 20th century and 27 of the 50 events in the 21st century. These potentially false outcomes occurred more frequently in Valonsadero (15%).

3.2. Reconstruction of Tree Management

There were identified 1588 pollarding events at tree level. The plot pollarding recurrence in the study area was 21 years (median value), with a range of 17 to 36 years (interquartile range, IQR). However, some consecutive events were spaced as much as 63 to 88 years apart (90th and 95th percentiles, P90 and P95). Pollarding was less recurrent Arguijo (a median of 27 years) than in the other studied sites (Rioseco = 20 years, Valonsadero = 21 years, and Vilviestre = 22 years) (Figure 2). The recurrence of pollarding was signifi-

cantly lower in the 20th and 21st centuries compared to earlier centuries across the study area. The decline in recurrence during the 21st century became more pronounced after excluding drought-related events (Figure 2 and Figure S2). At a decadal scale, pollarding was more recurrent (decade's median < site's median) during the periods 1560–1630, 1670, 1710, 1730, 1760–1810, 1860–1880, and 1900–1910 (Figure S3). In contrast, pollarding was less recurrent (decade's median > site's median) during 1640, 1720, 1750, 1920, 1940–1960, and 1980–2010. Excluding events potentially related to severe droughts in the 20th and 21st centuries, pollarding recurrence did not show relevant differences at a decadal scale compared to the initial reconstruction (Figure S3).

Pollarding led to a median reduction in tree radial growth for up to three years following the event, with a range of 2 to 4 years (IQR) (Figure S1). Less frequently, pollarding severity extended between 5 and 11 years (P90 and P99). Pollarding severity was generally lower in Rioseco (median: 2 years) compared to the other study sites (median: 3 years) (Figure 3). A significant negative temporal trend was observed only in Valonsadero during the study period, with pollarding in the 21st century being significantly less severe (median: 2 years) compared to previous centuries (median: 3 years). At a decadal scale, pollarding events in 1830, 1870, and 1940 were notably severe (decade's median > site's median) across the study area, while events in 1750, 1800, 1850, 1900, 1950, and 1990–2010 had lower severity (decade's median < site's median) (Figure S5). Excluding events potentially related to severe droughts in the 20th and 21st centuries, pollarding severity did not show significant differences at either the century (Figure S4) or decadal scale compared to the initial reconstruction (Figure S5).

Up to 14% of trees at each site were simultaneously affected by pollarding events (median value), with this proportion ranging from 8 to 25% (IQR). Less frequently, a single pollarding event impacted between 39 and 74% of the trees at a site (P90 and P99). Rioseco exhibited the most synchronous pollarding events (median: 35%), while Valonsadero showed the least (median: 11%). A significant overall decrease in pollarding synchrony was observed in Rioseco (Figure 4). In Arguijo, pollarding events in the 17th century were significantly more synchronous than in other centuries. In Vilviestre, the 18th century stands out for showing significantly lower synchrony compared to the others. A decline in synchrony was observed across the study area in the 21st century, as well as in Valonsadero once drought-related events were excluded (Figure 4 and Figure S6). At a decadal scale, pollarding events were more synchronous across the study area (decade's median > site's median) during the periods 1570–1610, 1640–1650, 1760–1800, 1940, and 1960 (Figure S7). Conversely, less synchronous pollarding events (decade's median < site's median) occurred during the decades of 1620–1630, 1670, 1700, 1830–1840, 1870, 1930, and 2000–2010. Excluding events potentially related to severe droughts in the 20th and 21st centuries, the decline in pollarding synchrony during the 2000s and 2010s became more pronounced (Figure S5).

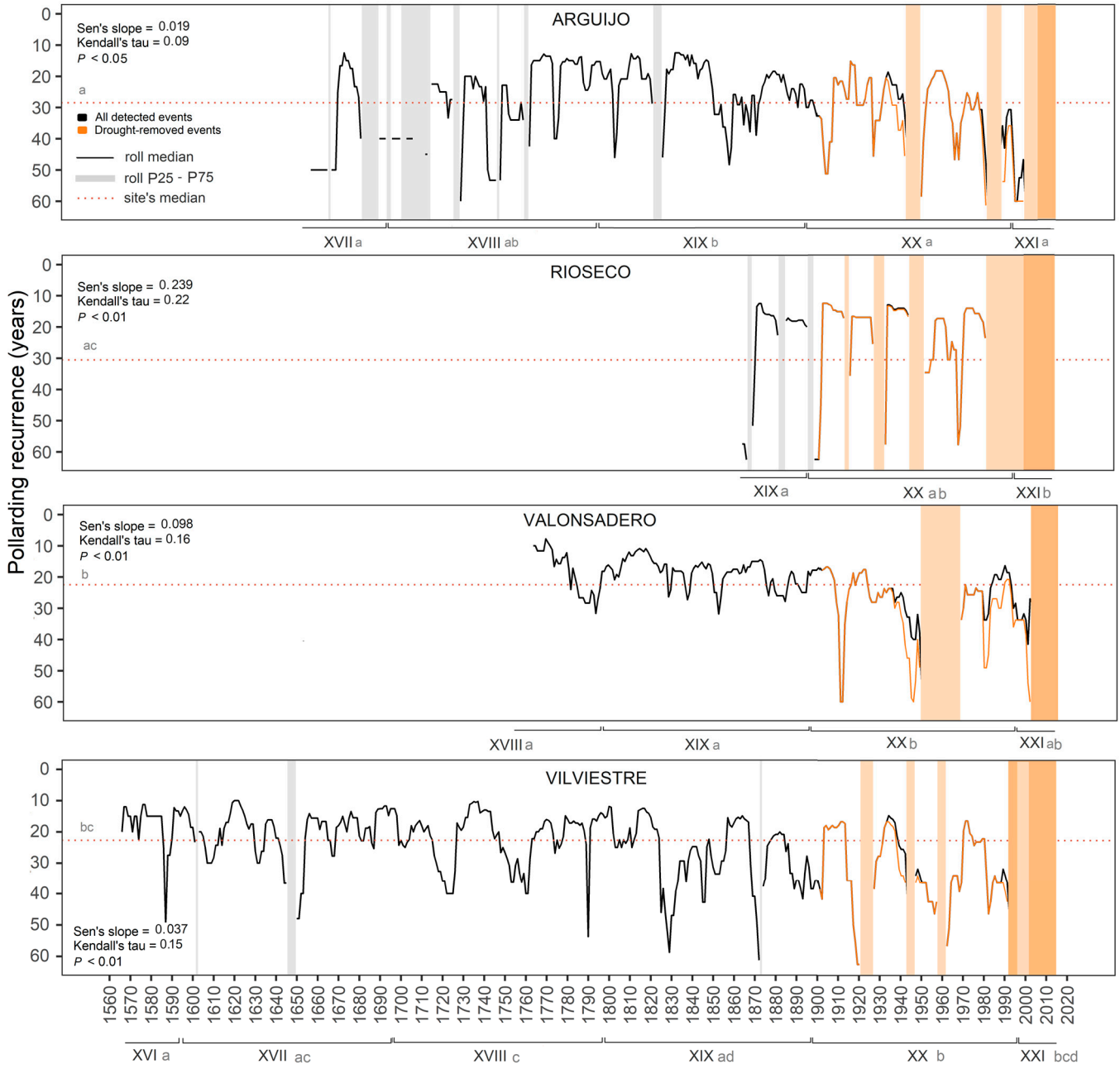

Figure 2. Temporal evolution of pollarding recurrence at the site level shown as a black solid line (computed for a 10-year anchored moving window at the focal year). The *y*-axis has been reversed for better interpretation, with a value of 1 year indicating the highest recurrence and infinity years indicating the least recurrence. The *y*-axis is truncated at the P90 value of the entire database (63 years). The gray-shaded periods highlight times when the recurrence values exceed this truncation threshold. Bars represent the number of pollarding events by decade at each site, centered by decade. The overall median of the site is shown as a red dotted line. Each panel corresponds to one study site. Statistical differences between sites and centuries are indicated by different letters (Dunn test, $p < 0.05$). The results of the temporal trend analysis are displayed in the top-left corner. The additional orange line represents recurrence data for the 20th and 21st centuries, excluding the potential confounding effect of severe droughts.

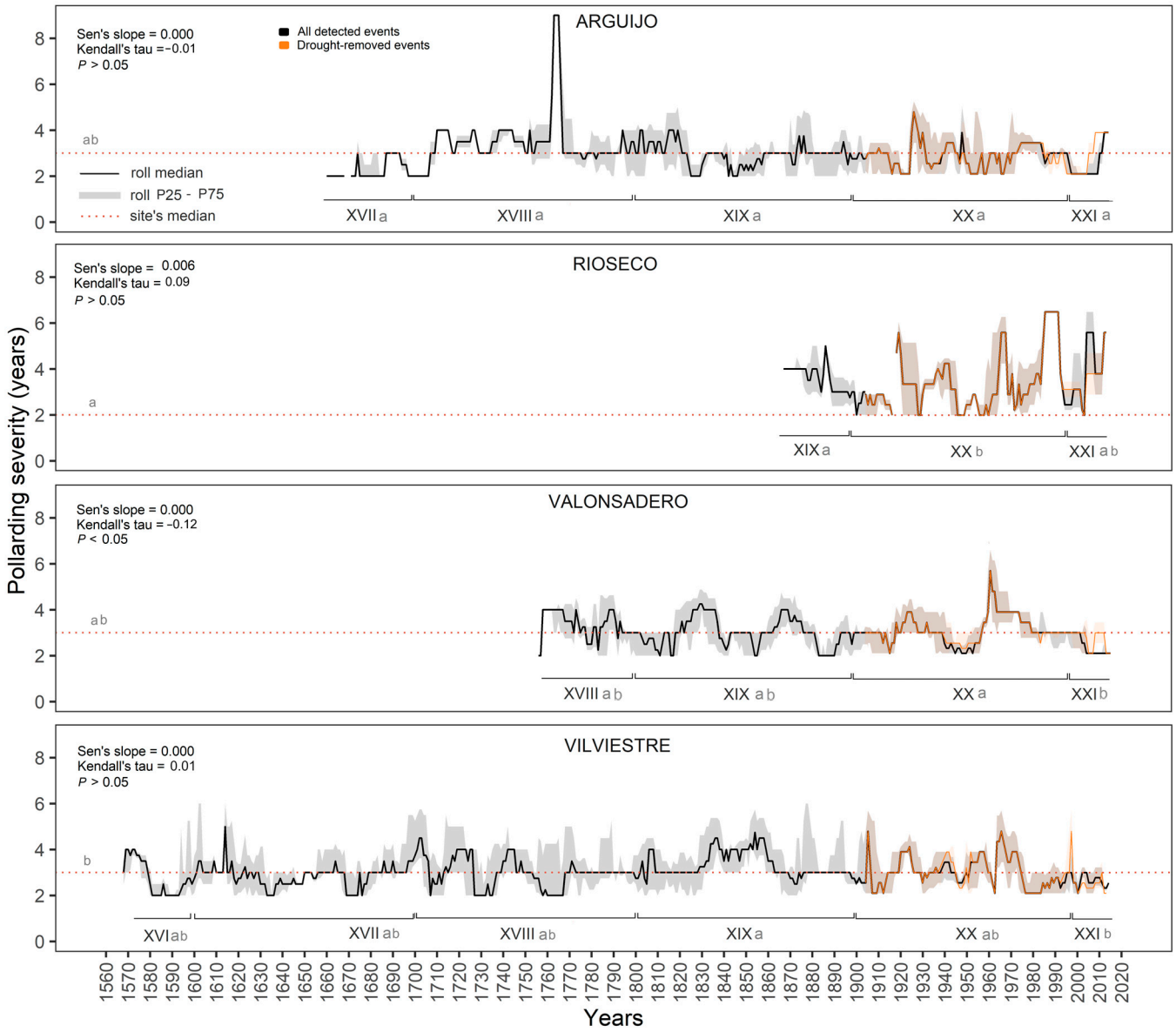

Figure 3. Temporal evolution of pollarding severity (smoothed using a 10-year rolling median) shown as a black solid line. The overall median of the site is shown as a red dotted line. Shaded area indicates the interquartile range (smoothed using a 10-year rolling P25 and P75). Each panel corresponds to one study site. Statistical differences between sites and centuries are indicated by different letters (Dunn test, $p < 0.05$). The results of the temporal trend analysis are displayed in the top-left corner. The additional orange line represents severity data for the 20th and 21st centuries, excluding the potential confounding effect of severe droughts.

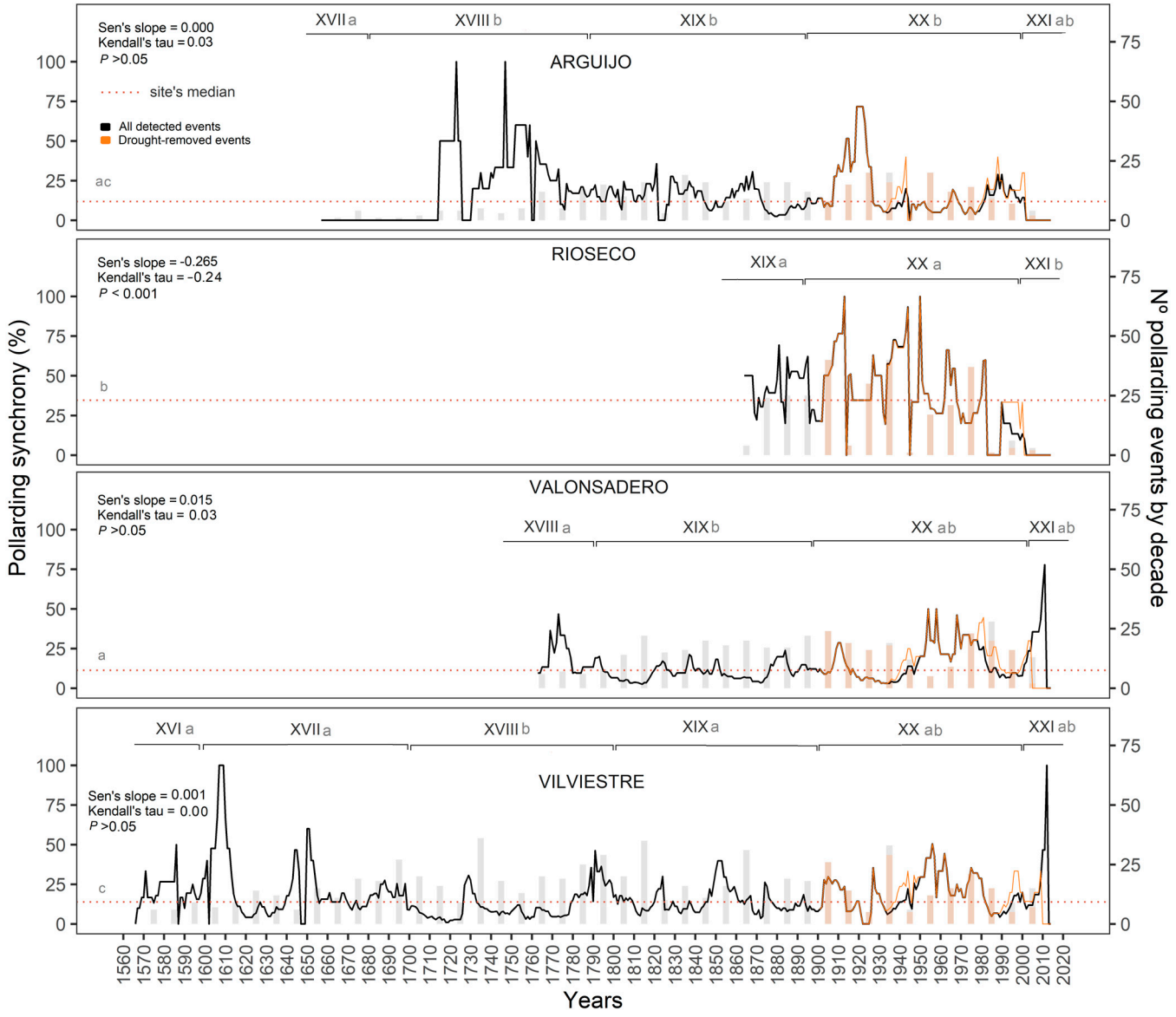

Figure 4. Temporal evolution of pollarding synchrony shown as a black solid line (computed for 10-year anchored moving window at focal year, at site level). Maximal synchrony is represented at a value of 100. Bars show the number of pollarding events by decade at each site, centered by decade. The overall median of the site is shown as a red dotted line. Each panel corresponds to one study site. Statistical differences between sites and centuries are indicated by different letters (Dunn test, $p < 0.05$). The results of the temporal trend analysis are displayed in the top-left corner. The additional orange line represents synchrony data for the 20th and 21st centuries, excluding the potential confounding effect of severe droughts.

3.3. Differential Radial-Growth Responses to Pollarding

The typical duration of pollarding effects usually lasted 3 years, as previously mentioned. Pollarding events led to a significant reduction in RW, with median decreases of 28% in the first year after pollarding, 38% in the second year, and 48% in the third year (Figure 5). This reduction was primarily due to a significant decrease in LW production, with median reductions of 58%, 73%, and 84%, respectively. In contrast, EW production did not show any reduction in the first year (0%) but exhibited a lower yet significant median decrease of 6% and 13% in the second and third years, respectively.

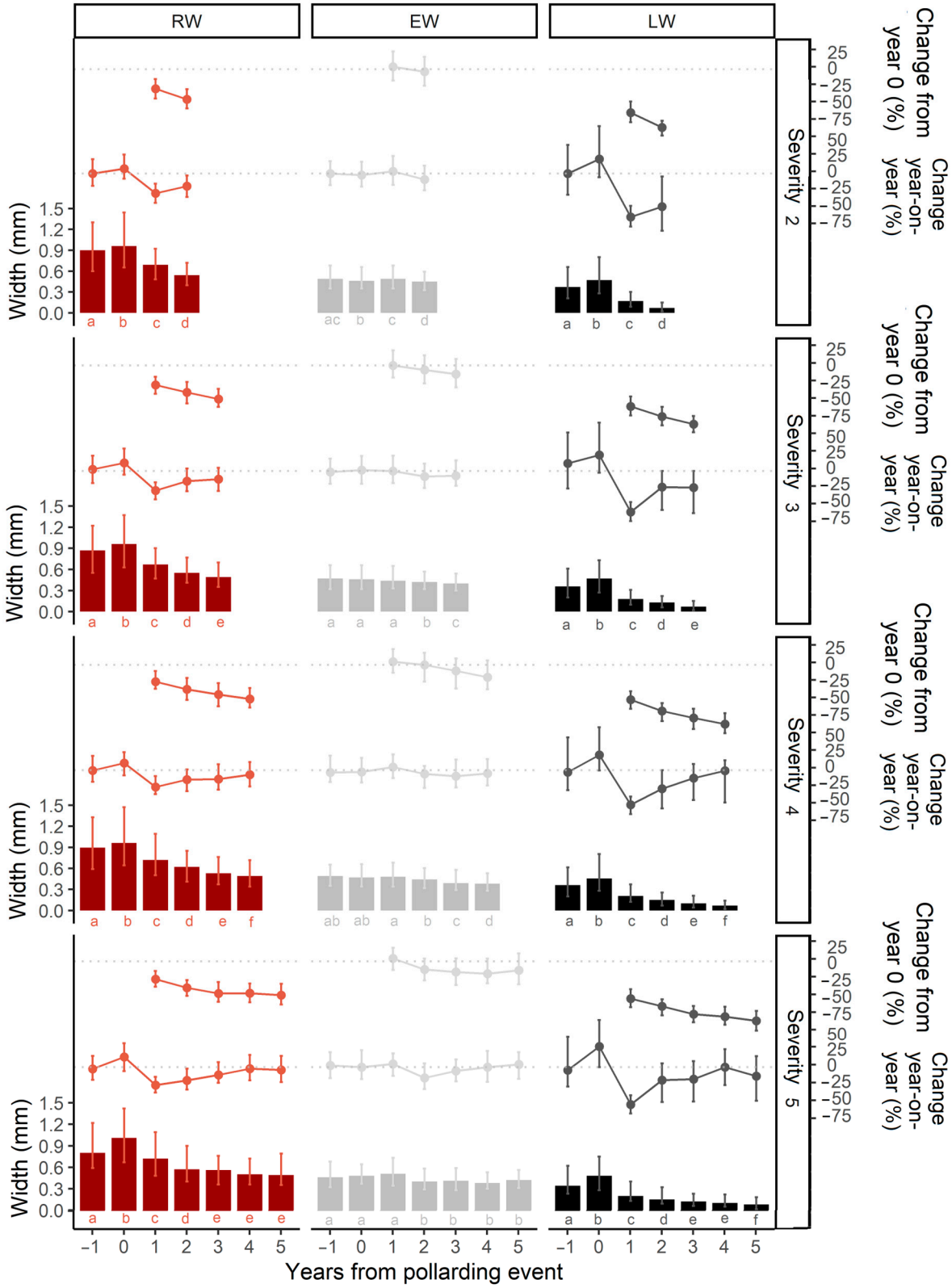

Figure 5. Year-on-year change in ring width (RW), earlywood (EW), and latewood (LW) from one year before pollarding to five years after in primary pollarding events (bar charts). The upper line chart displays the percentage change relative to the pre-pollarding conditions (year 0). The lower line chart displays the year-on-year percentage change. Time span covers the most common number of years in which the effects of pollarding were observed (P90 = 5 years). Columns or dots represent the median; whiskers indicate the interquartile range. Statistical differences between years are indicated by different letters (Wilcoxon test for paired samples, $p < 0.05$).

Pollarding events, when categorized by their severity, resulted in significantly different magnitudes of post-pollarding growth reduction in terms of RW and LW (RW: Z = 9.54; LW: Z = 32.22; $p < 0.05$) (Figure 5). A severity of 2 years produced the most significant reduction in LW during the first and second year after pollarding compared to pre-pollarding conditions (median: 62 and 84%, respectively). A severity of 3 years resulted in the greatest significant reduction in both RW and LW during the third year after pollarding (median: 48 and 84%, respectively). Finally, a severity of 4 years led to the most significant reduction in RW and LW during the fourth year after pollarding (median: 49 and 84%, respectively).

Most pollarding events consisted of isolated occurrences taking place at least two years after the effects of the previous pollarding event have ceased (Figure 5). However, we identified a secondary type of practice, which accounted for only 5% of cases, involving concatenated events occurring immediately in the year following the cessation of the effects from the previous pollarding event (Figure S8). Secondary events exhibited a significantly greater overall reduction in LW (+8%; Z = 15.72; $p < 0.01$) relative to pre-pollarding conditions compared to primary events when analyzing the most common period of observed pollarding effects (up to 5 years) without distinguishing events by severity type. However, when distinguishing events by severity type, these differences were significant only in specific cases, primarily due to the scarcity of samples for secondary pollarding (Figure S8).

No significant differences have been observed in the responses of the sampled species to pollarding, including the duration of the pollarding effect (severity) (Z = 2.63; $p > 0.05$) and percentage changes in RW (Z = 0.90; $p > 0.05$), EW (Z = 2.32; $p > 0.05$), and LW (Z = 2.28; $p > 0.05$) relative to pre-pollarding conditions. This holds when analyzing the most common period of observed pollarding effects (up to 5 years), both with and without distinguishing events by severity type.

4. Discussion and Conclusions

To the best of our knowledge, this is the first reconstruction of historical pollarding practices using a semi-automatic machine learning algorithm. These events primarily led to a reduction in latewood production, typically lasting three years, with the most significant decreases occurring towards the end of the pollarding effect period. The median pollarding recurrence was 21 years, although this varied significantly between sites and sharply decreased across the study area since the last third of the 20th century. The key historical decades of high and low pollarding pressure were common in all studied *dehesas* in north-central Spain, suggesting a common socioeconomic driver.

Our random forest model successfully identified 85% of the pollarding events used in training. However, it tended to misclassify certain severe droughts as pollarding events. The model's performance declined in the late 20th and early 21st centuries, where severe droughts and branch breakage due to the cessation of management were often confused with pollarding. Further refinement is possible by expanding the training dataset and incorporating additional parameters, such as vessel size distribution, to reduce false positives [21].

The detection of pollarding events has traditionally relied on methods developed to identify radial-growth suppressions and releases primarily designed for tree-to-tree competition modulated forests. These methods, such as the radial-growth averaging criteria [38], typically use ten-year temporal windows [10,18,19,24]. Our findings demonstrated that the effects of pollarding are much shorter, leading to growth reductions primarily lasting 2–4 years. This underscores the importance of using short-term predictors (less than 5 years) based on latewood features to accurately identify pollarding events since the proportion of earlywood remains unchanged for some time. When a tree is pollarded and experiences extensive loss of photosynthetic tissues, it enters a growth-limiting condition that prioritizes functions essential for survival. As a result, latewood production is more affected than earlywood production. Earlywood is crucial for hydraulic transport, which is

vital for the tree's survival, whereas latewood primarily serves a mechanical function that is less relevant in a tree without canopy [54].

The pollarding impact observed, characterized by a sudden reduction in ring width lasting about 3 years followed by a gradual recovery, has been termed the "loss-of-crown-type" pattern [55], aligning with previous studies [20,21,23]. A key finding of our study is that maximum impact on tree growth was not reached immediately after the disturbance. Instead, it gradually intensified, reaching a maximum before recovery begins, regardless of the duration of the impact (Figure 5). Ring-width reduction, compared to pre-pollarding levels, increased gradually from 28% in the first year to 38% in the second and 48% in the third year. This decline in ring-width was mainly due to a significant decrease in latewood production [20,21,23] (58%, 73%, and 84% from the first to the third year), while earlywood production remained stable in the first year and showed only modest declines in the second (6%) and third years (13%). This pattern may reflect the use of substantial carbohydrate pools during the initial years following the pollarding [22] and possibly an allometric effect related to increasing demands for canopy recovery as branches grow. We hypothesize that the end of the radial-growth reduction caused by pollarding and the beginning of recovery could represent the compensation point between canopy carbon demands and production.

Detecting pollarding events allowed for a long-term reconstruction of management patterns in the studied *dehesas* and the identification of distinct pollarding practices. The median pollarding interval was 21 years, suggesting that the practice was primarily aimed at producing timber, charcoal, or firewood, as this interval typically ranges from 10 to 76 years in deciduous oaks [19,56]. Additionally, we identified a secondary pollarding method, accounting for 5% of the detected events, involving a second pruning one year after the onset of latewood recovery, when branches are still small. This method, known as *olivado*, was aimed at obtaining fodder because young branches are easy to cut and highly valued by livestock during the summer months when pastures are scarce [57].

Tree growth reconstructions have often been used to assess historical population dynamics [58,59]. The historical reconstruction of *dehesas* management in north-central Spain conducted in this study can be broadly contextualized within the region's socioeconomic transformation. In the 16th century, Spain experienced a population increase that intensified pressure on woodlands from peasants, stockmen, and urban dwellers seeking fuel and timber [60]. The studied *dehesas* underwent intense exploitation from the 1560s to the early 17th century, characterized by the high recurrence and synchrony of pollarding. In contrast, the 17th century saw a decline in population due to wars and diseases, leading to a steady decrease in agriculture and significant rural depopulation [60,61]. During this period, the studied *dehesas* did not display a common management pattern, with recurrence varying between decades. The 18th century witnessed a population increase that led to increased pressure on the land, marked by a new management model that prohibited transhumant grazing and promoted the use of uncultivated land for timber production [9]. In this period, the studied *dehesas* showed dominant high recurrence of pollarding throughout the century (1710s, 1730s, and from 1760s to early 19th century), with the last decades also characterized by high synchrony. In the 19th century and early 20th century, the demand for agricultural and forest products, such as charcoal from oaks, increased alongside population growth and industrial development [61]. In the studied *dehesas*, in addition to the period of intense exploitation pressure noted at the beginning of the 18th century, the end of that century and the beginning of the 19th century are also significant for the same reason, characterized by recurrent pollarding events. Following the Spanish Civil War (1936–1939), the recurrence of pollarding declined across the study area.

During the second half of the 20th century, the management of communal deciduous oak *dehesas* largely ceased across Spain. In the 1960s and early 1970s, Spain transitioned from an underdeveloped to a developed country [62], leading to massive rural depopulation and the collapse of traditional practices from that time [63]. In the *dehesas* of north-central Spain that were studied, this decline was particularly pronounced in the third part of the century, becoming even more notable in the 21st century, marked by a sharp reduction in pollarding

recurrence, severity, and synchrony. This reflects a shift in pollarding practices, transitioning from traditional to modern approaches and in some cases resulting in a complete cessation of pollarding. In the Arguijo and Vilviestre sites, the most recent pollarding events detected are the result of the efforts of individual managers and environmental agents attempting to revive this practice to preserve tree integrity (JM Olano pers obs). The events detected by the model in the other two *dehesas* during the 21st century may be associated with severe droughts and branch breakage resulting from lack of management, as no pollarding has occurred.

Wars, property changes, and societal factors have historically impacted *dehesa* management, sometimes leading to tree logging or even the disappearance of entire *dehesas* [60]. Despite these losses, the *dehesas* in this study have persisted for centuries, as evidenced by the long lifespan of the trees. Pollarding provided sustainable wood extraction without the need for further logging, as branches were more productive than trunks, and compatible with livestock management, incidentally, contributing to the preservation of ancient trees.

The findings of this study are crucial for guiding conservation strategies that preserve the ecological and cultural integrity of northern Iberian *dehesas*. Restoring pollarding in areas where it has been abandoned is essential, despite the challenges of continuing traditional pollarding practices due to rural depopulation and the shift to alternative biomass sources. Under certain conditions, however, large-scale pollarding could be economically viable. In all cases, sustaining this management practice is essential for preserving the biodiversity associated with this priority habitat. The recurrence and average severity of pollarding observed over the past four centuries in this study could serve as guidelines for re-establishing pollarding practices, as this management pattern has been pivotal in their survival to the present day. The current lack of management, coupled with the increasing frequency of drought stress, has led to severe tree dieback and accelerated aging of tree physiology in Iberian *dehesas* [10,64]. The methodologies developed here could be applied to another regions, enhancing our understanding of the historical management of deciduous oak open woodlands. Superposed epoch analysis could also be considered a potential method for investigating conditions before and after pollarding events in relation to relative tree-ring growth. Future research should focus on refining machine learning models to better distinguish between pollarding and environmental stressors such as drought, possibly by incorporating additional dendrological variables. This refinement will facilitate a deeper understanding of these forests' climate responses, recognizing their significant potential in this area [17].

Supplementary Materials: The following supporting information can be downloaded at: https://www.mdpi.com/article/10.3390/f15122090/s1, Table S1: Predictor variables considered in the model; Table S2: Lag and month with the highest correlation (R^2) between SPEI values and the mean latewood width index value chronology of each study site; Figure S1: Examples of the signals produced by different intensities of pollarding; Figure S2: Pollarding recurrence by site and century, comparing all detected events with those excluding potential severe droughts; Figure S3: Frequency with which decades of the same pollarding recurrence level were common to the four studied sites; Figure S4: Pollarding severity by site and century, comparing all detected events with those excluding potential severe droughts; Figure S5: Frequency with which decades of the same pollarding severity level were common to the four studied sites; Figure S6: Pollarding synchrony by site and century, comparing all detected events with those excluding potential severe droughts; Figure S7: Frequency with which decades of the same pollarding synchrony level were common to the four studied sites; Figure S8: Differential latewood responses to pollarding between primary and secondary types of events.

Author Contributions: Conceptualization, A.S.-V., G.S.-B., M.G.-H. and J.M.O.; fieldwork: J.M.O., G.S.-B. and M.G.-H.; cross-dating: J.M.O.; methodology, A.S.-V.; software, M.G.-H.; validation, A.S.-V., G.S.-B., M.G.-H. and J.M.O.; formal analysis, A.S.-V.; investigation, all authors; resources, J.M.O. and G.S.-B.; data curation, A.S.-V., M.E.C. and J.M.O.; writing—original draft preparation, A.S.-V., G.S.-B. and J.M.O.; writing—review and editing, all authors; visualization, A.S.-V.; supervision, J.M.O. and

G.S.-B.; project administration, J.M.O. and G.S.-B.; funding acquisition, J.M.O. and G.S.-B. All authors have read and agreed to the published version of the manuscript.

Funding: This research was funded by the project GIANTS (PID2023-147214NB-I00) funded by MICIU/AEI/10.13039/501100011033 and FEDER, UE. A.S.-V. was supported by a postdoctoral grant JDC2022-048316-I funded by MICIU/AEI/10.13039/501100011033 and by European Union NextGenerationEU/PRTR.

Data Availability Statement: Data will be made available upon request.

Acknowledgments: We would like to thank the "Servicio de Medio Ambiente de la Junta de Castilla y León" and especially José Antonio Lucas for providing the sampling permissions and the managers and environmental agents for providing sample information on the sites and their management. Juan Carlos Rubio and Alfonso Martínez provided invaluable help for sample preparation. We extend our gratitude for assistance with the fieldwork to Maru García, Vicente Rozas, Héctor Hernández, Lorena Caiza, Elena Moreno, David Candel, Hermine Houdas, and Javier Durá. A.S.V. sincerely thanks Sergio García for the supervision of the statistical methods.

Conflicts of Interest: The authors declare no conflicts of interest. The funders had no role in the design of this study; in the collection, analyses, or interpretation of data; in the writing of the manuscript; or in the decision to publish the results.

References

1. Petit, S.; Watkins, C. Pollarding Trees: Changing Attitudes to a Traditional Land Management Practice in Britain 1600–1900. *Rural. Hist.* **2003**, *14*, 157–176. [CrossRef]
2. Butler, J. Looking Back to the Future: Ancient, Working Pollards and Europe's Silvo-Pastoral Systems. In *Cultural Severance and the Environment: The Ending of Traditional and Customary Practice on Commons and Landscapes Managed in Common*; Rotherham, I.D., Ed.; Springer Netherlands: Dordrecht, The Netherlands, 2013; pp. 371–376. ISBN 978-94-007-6159-9.
3. Harrison, R. Arboriculture in South West Europe: Dehesas as Managed Woodlands. In *The Origins and Spread of Agriculture and Pastoralism in Eurasia*; Routledge: London, UK, 1996; pp. 363–367.
4. Chavan, S.B.; Kumar, N.; Uthappa, A.R.; Keerthika, A.; Handa, A.K.; Sridhar, K.B.; Singh, M.; Kumar, D.; Ram, N. Tree Management Practices in Agroforestry. In *Forests, Climate Change and Biodiversity*; Sood, K.K., Mahajan, V., Eds.; Kalyani Publishers: New Delhi, India, 2018; pp. 87–101.
5. Moreno, G.; López-Díaz, M.L. The Dehesa: The Most Extensive Agroforestry System in Europe. *Agrofor. Syst. A Tech. Sustain. Land Manag.* **2009**, 171.
6. San Miguel Ayanz, A. *La Dehesa Española: Orígen, Tipología, Características y Gestión*; Fundación Conde del Valle de Salazar: Madrid, India, 1994; ISBN 978-84-86793-24-1.
7. Corominas, J. *Diccionario Crítico Etimológico de La Lengua Castellana*; Editorial Gredos: Madrid, Spain, 1954.
8. Rodríguez Pascual, M. *La Trashumancia. Cultura, Cañadas y Viajes*; Edilesa: León, Spain, 2001.
9. Vicente, Á.M.; Alés, R.F. Long Term Persistence of Dehesas. Evidences from History. *Agroforest Syst.* **2006**, *67*, 19–28. [CrossRef]
10. Colangelo, M.; Valeriano, C.; De Andrés, E.G.; Pizarro, M.; Murria, E.; Julio Camarero, J. Lack of Management, Land-Use Changes, Poor Site Conditions and Drought Contribute to the Decline of Old Pollarded Oaks. *Dendrochronologia* **2024**, *86*, 126232. [CrossRef]
11. Pérez, R.; Salinas, V. *Keys to the Recognition of the Dehesa as UNESCO Cultural Landscape*; Univ Complutense Madrid: Madrid, Spain, 2015; Volume 35, pp. 121–142.
12. Silva Pérez, M.R. *La Dehesa Vista Como Paisaje Cultural. Fisonomías, Funcionalidades y Dinámicas Históricas. Ería: Revista Cuatrimestral de Geografía*; Gredos: Madrid, Spain, 2010; Volume 82, pp. 143–157.
13. García-Tejero, S.; Taboada, Á.; Tárrega, R.; Salgado, J.M. Land Use Changes and Ground Dwelling Beetle Conservation in Extensive Grazing Dehesa Systems of North-West Spain. *Biol. Conserv.* **2013**, *161*, 58–66. [CrossRef]
14. Sebek, P.; Altman, J.; Platek, M.; Cizek, L. Is Active Management the Key to the Conservation of Saproxylic Biodiversity? Pollarding Promotes the Formation of Tree Hollows. *PLoS ONE* **2013**, *8*, e60456. [CrossRef]
15. Brienen, R.J.; Caldwell, L.; Duchesne, L.; Voelker, S.; Barichivich, J.; Baliva, M.; Ceccantini, G.; Di Filippo, A.; Helama, S.; Locosselli, G.M. Forest Carbon Sink Neutralized by Pervasive Growth-Lifespan Trade-Offs. *Nat. Commun.* **2020**, *11*, 4241. [CrossRef]
16. Lonsdale, D.; Pollarding Success or Failure. Some Principles to Consider. In *Pollard and Veteran Tree Management II, Corporation of London, Burnham Beeches*; Read, H.J., Ed.; The Richmond Publishing Company: London, UK, 1996; pp. 100–104.
17. Olano, J.M.; García-López, M.A.; Sangüesa-Barreda, G.; Coca, M.E.; García-Hidalgo, M.; Houdas, H.; Rozas, V.; Hernández-Alonso, H. Forgotten Giants: Robust Climate Signal in Pollarded Trees. *Sci. Total Environ.* **2023**, *903*, 166591. [CrossRef]
18. Camarero, J.J.; González de Andrés, E.; Colangelo, M.; de Jaime Loren, C. Growth History of Pollarded Black Poplars in a Continental Mediterranean Region: A Paradigm of Vanishing Landscapes. *For. Ecol. Manag.* **2022**, *517*, 120268. [CrossRef]
19. Rozas, V. A Dendroecological Reconstruction of Age Structure and Past Management in an Old-Growth Pollarded Parkland in Northern Spain. *For. Ecol. Manag.* **2004**, *195*, 205–219. [CrossRef]

20. Rozas, V. Dendrochronology of Pedunculate Oak (*Quercus Robur* L.) in an Old-Growth Pollarded Woodland in Northern Spain: Establishment Patterns and the Management History. *Ann. For. Sci.* **2005**, *62*, 13–22. [CrossRef]
21. Bernard, V.; Renaudin, S.; Marguerie, D. Evidence of Trimmed Oaks (*Quercus* Sp.) in North Western France during the Early Middle Ages (9th–11th Centuries AD). *Charcoal Anal. New Anal. Tools Methods Archaeology. BAR Int Ser* **2006**, *1483*, 103–108.
22. Bleicher, N. Four Levels of Patterns in Tree-Rings: An Archaeological Approach to Dendroecology. *Veget Hist Archaeobot* **2014**, *23*, 615–627. [CrossRef]
23. Schweingruber, F.H. Modification of the Tree-Ring Structure Due to Defoliation and Pollarding. In *Wood Structure and Environment*; Schweingruber, F.H., Ed.; Springer Series in Wood Science; Springer: Berlin, Heidelberg, 2007; pp. 139–178. ISBN 978-3-540-48548-3.
24. Camarero, J.J.; Valeriano, C. Responses of Ancient Pollarded and Pruned Oaks to Climate and Drought: Chronicles from Threatened Cultural Woodlands. *Sci. Total Environ.* **2023**, *883*, 163680. [CrossRef]
25. Jevšenak, J.; Džeroski, S.; Zavadlav, S.; Levanič, T. A Machine Learning Approach to Analyzing the Relationship Between Temperatures and Multi-Proxy Tree-Ring Records. *Tree-Ring Res.* **2018**, *74*, 210–224. [CrossRef]
26. Li, J.; Wang, Z.; Lai, C.; Zhang, Z. Tree-Ring-Width Based Streamflow Reconstruction Based on the Random Forest Algorithm for the Source Region of the Yangtze River, China. *Catena* **2019**, *183*, 104216. [CrossRef]
27. Pavão, D.C.; Jevšenak, J.; Silva, L.B.; Elias, R.B.; Silva, L. Climate–Growth Relationships in Laurus Azorica—A Dominant Tree in the Azorean Laurel Forest. *Forests* **2023**, *14*, 166. [CrossRef]
28. Liu, Z.; Peng, C.; Work, T.; Candau, J.-N.; Desrochers, A.; Kneeshaw, D. Application of Machine-Learning Methods in Forest Ecology: Recent Progress and Future Challenges. *Environ. Rev.* **2018**, *26*, 339–350. [CrossRef]
29. Caudullo, G.; Welk, E.; San-Miguel-Ayanz, J. Chorological Maps for the Main European Woody Species. *Data Brief* **2017**, *12*, 662–666. [CrossRef]
30. García-Hidalgo, M.; García-Pedrero, Á.; Colón, D.; Sangüesa-Barreda, G.; García-Cervigón, A.I.; López-Molina, J.; Hernández-Alonso, H.; Rozas, V.; Olano, J.M.; Alonso-Gómez, V. CaptuRING: A Do-It-Yourself Tool for Wood Sample Digitization. *Methods Ecol. Evol.* **2022**, *13*, 1185–1191. [CrossRef]
31. Bunn, A.G. A Dendrochronology Program Library in R (dplR). *Dendrochronologia* **2008**, *26*, 115–124. [CrossRef]
32. R Core Team. *R: A Language and Environment for Statistical Computing*; R Foundation for Statistical Computing: Vienna, Austria, 2023.
33. Breiman, L. Random Forests. *Mach. Learn.* **2001**, *45*, 5–32. [CrossRef]
34. Liaw, A.; Wiener, M. Classification and Regression by randomForest. *R News* **2002**, *2*, 18–22.
35. Svetnik, V.; Liaw, A.; Tong, C.; Culberson, J.C.; Sheridan, R.P.; Feuston, B.P. Random Forest: A Classification and Regression Tool for Compound Classification and QSAR Modeling. *J. Chem. Inf. Comput. Sci.* **2003**, *43*, 1947–1958. [CrossRef] [PubMed]
36. Rossi, S.; Deslauriers, A.; Griçar, J.; Seo, J.-W.; Rathgeber, C.B.; Anfodillo, T.; Morin, H.; Levanic, T.; Oven, P.; Jalkanen, R. Critical Temperatures for Xylogenesis in Conifers of Cold Climates. *Glob. Ecol. Biogeogr.* **2008**, *17*, 696–707. [CrossRef]
37. Sahour, H.; Gholami, V.; Torkaman, J.; Vazifedan, M.; Saeedi, S. Random Forest and Extreme Gradient Boosting Algorithms for Streamflow Modeling Using Vessel Features and Tree-Rings. *Env. Earth Sci* **2021**, *80*, 747. [CrossRef]
38. Nowacki, G.J.; Abrams, M.D. Radial-Growth Averaging Criteria for Reconstructing Disturbance Histories from Presettlement-Origin Oaks. *Ecol. Monogr.* **1997**, *67*, 225–249. [CrossRef]
39. Oshiro, T.M.; Perez, P.S.; Baranauskas, J.A. How Many Trees in a Random Forest? In Proceedings of the Machine Learning and Data Mining in Pattern Recognition; Perner, P., Ed.; Springer: Berlin/Heidelberg, Germany, 2012; pp. 154–168.
40. Beguería, S.; Vicente-Serrano, S.M. SPEI: Calculation of the Standardized Precipitation-Evapotranspiration Index. Version 1.8.1. 2023. Available online: https://github.com/sbegueria/SPEI (accessed on 12 October 2024).
41. Vicente-Serrano, S.M.; Beguería, S.; López-Moreno, J.I. A Multiscalar Drought Index Sensitive to Global Warming: The Standardized Precipitation Evapotranspiration Index. *J. Clim.* **2010**, *23*, 1696–1718. [CrossRef]
42. Harris, I.; Osborn, T.J.; Jones, P.; Lister, D. Version 4 of the CRU TS Monthly High-Resolution Gridded Multivariate Climate Dataset. *Sci. Data* **2020**, *7*, 109. [CrossRef]
43. Agnew, C.T. *Using the SPI to Identify Drought*; University of Nebraska Lincoln: Lincoln, NE, USA, 2000; Volume 12.
44. Tonelli, E.; Vitali, A.; Brega, F.; Gazol, A.; Colangelo, M.; Urbinati, C.; Camarero, J.J. Thinning Improves Growth and Resilience after Severe Droughts in *Quercus Subpyrenaica* Coppice Forests in the Spanish Pre-Pyrenees. *Dendrochronologia* **2023**, *77*, 126042. [CrossRef]
45. Candel-Pérez, D.; Hernández-Alonso, H.; Castro, F.; Sangüesa-Barreda, G.; Mutke, S.; García-Hidalgo, M.; Rozas, V.; Olano, J.M. 250-Year Reconstruction of Pollarding Events Reveals Sharp Management Changes in Iberian Ash Woodlands. *Trees* **2022**, *36*, 1909–1921. [CrossRef]
46. Altman, J.; Fibich, P.; Dolezal, J.; Aakala, T. TRADER: A Package for Tree Ring Analysis of Disturbance Events in R. *Dendrochronologia* **2014**, *32*, 107–112. [CrossRef]
47. Druckenbrod, D.L.; Cook, E.R.; Pederson, N.; Martin-Benito, D. Detrending Tree-Ring Widths in Closed-Canopy Forests for Climate and Disturbance History Reconstructions. *Dendrochronologia* **2024**, *85*, 126195. [CrossRef]
48. Kruskal, W.H.; Wallis, W.A. Use of Ranks in One-Criterion Variance Analysis. *J. Am. Stat. Assoc.* **1952**, *47*, 583–621. [CrossRef]
49. Dunn, O.J. Multiple Comparisons Using Rank Sums. *Technometrics* **1964**, *6*, 241–252. [CrossRef]
50. Kendall, M.G. *Rank Correlation Methods*; Griffin: Hackensack, NJ, USA, 1948.

51. Mann, H.B. Nonparametric Tests Against Trend. *Econometrica* **1945**, *13*, 245. [CrossRef]
52. Sen, P.K. Estimates of the Regression Coefficient Based on Kendall's Tau. *J. Am. Stat. Assoc.* **1968**, *63*, 1379–1389. [CrossRef]
53. Bronaugh, D.; Werner, A.; Bronaugh, M.D. Package 'zyp'. CRAN Repository. Version 0.11-1. Available online: https://cran.hafro.is/web/packages/zyp/zyp.pdf (accessed on 12 October 2024).
54. Domec, J.-C.; Gartner, B.L. How Do Water Transport and Water Storage Differ in Coniferous Earlywood and Latewood? *J. Exp. Bot.* **2002**, *53*, 2369–2379. [CrossRef]
55. Guibal, F.; Bernard, V. Approche Dendrochronologique de l'évolution Récente Du Système Bocager Armoricain. In *Annales Literaires*; Dialogues d'histoire ancienne; Universite de Besancon: Besancon, France, 2002; Volume 730, pp. 463–472.
56. Haneca, K.; Katarina, Čufar; Beeckman, H. Oaks, Tree-Rings and Wooden Cultural Heritage: A Review of the Main Characteristics and Applications of Oak Dendrochronology in Europe. *J. Archaeol. Sci.* **2009**, *36*, 1–11. [CrossRef]
57. Gómez Gutiérrez, J.M. *El Libro de Las Dehesas Salmantinas*; Junta de Castilla y León: Valladolid, Spain, 1992.
58. Chen, F.; Man, W.; Wang, S.; Esper, J.; Meko, D.; Büntgen, U.; Yuan, Y.; Hadad, M.; Hu, M.; Zhao, X.; et al. Southeast Asian Ecological Dependency on Tibetan Plateau Streamflow over the Last Millennium. *Nat. Geosci.* **2023**, *16*, 1151–1158. [CrossRef]
59. Bellorado, B.A.; Windes, T.C. Revisiting the Depopulation of the Northern Southwest with Dendrochronology. In *Research, Education and American Indian Partnerships at the Crow Canyon Archaeological Center*; University Press of Colorado: Denver, CO, USA, 2023; p. 282.
60. Álvarez, J.R.G. The Image of a Tamed Landscape: dehesa</Em> through History in Spain. *Cult. Hist. Digit. J.* **2016**, *5*, e003. [CrossRef]
61. Domínguez Ortiz, A.; Cortés Peña, A.L. *La Sociedad Española En El Siglo XVII.*; Archivum; Edición facsímil; Universidad de Granada: Granada, Spain, 1992.
62. Petrovic, R. Spanish Economic Miracle between 1959 to 1973. *ODITOR* **2020**, *2020*, 66. [CrossRef]
63. Collantes, F.; Pinilla, V. *Peaceful Surrender: The Depopulation of Rural Spain in the Twentieth Century*; Cambridge Scholars Publishing: Cambridge, UK, 2011; ISBN 978-1-4438-3136-9.
64. Cantero, A. *Apuntes Sobre Trasmochos: Guía de Buenas Prácticas Para el Trasmocheo*; Gipuzkoako Foru Aldundia = Diputación Foral de Guipúzcoa: Donostia, Spain, 2014.